CHEMISTRY
A EUROPEAN JOURNAL

DOI: 10.1002/chem.200600084

Absolute Configuration of New Cytotoxic and Other Bioactive Trichothecene Macrolides

Li Shen[†], Rui H. Jiao[†], Yong H. Ye, Xiao T. Wang, Chen Xu, Yong C. Song, Hai L. Zhu,* and Ren X. Tan*[a]

Abstract: Three new cytotoxic 10,13-cyclotrichothecane-derived macrolides, myrothecines A–C (**1**–**3**), were characterized from the extracts of two *Myrothecium roridum* strains, IFB-E009 and IFB-E012, isolated as endophytic fungi found on the traditional Chinese medicinal plants *Trachelospermum jasminoides* and *Artemisia annua*, respectively. The absolute configuration of myrothecines A–C was elucidated by a combination of spectral techniques (UV, IR, MS, circular dichroism (CD), ^{1}H and ^{13}C NMR, DEPT, ^{1}H–^{1}H COSY, NOESY, HMQC, and HMBC spectrascopic analyses), Mosher's ester analysis, and single-crystal X-ray diffraction. The absolute configuration of the reported bioactive analogue, mytoxin B was established by correlating its spectral data with that of known absolute configurational structures. Furthermore, the significance in endophytism (or symbiosis) and biocatabolism, highlighted by production of those macrolides by the endophytic strains, is discussed in brief.

Keywords: endophyte · myrothecine · natural products · structure elucidation · total synthesis

Introduction

Trichothecenes are structurally a family of fungi-produced sesquiterpenols with or free of acyl residue(s). Among this type of secondary metabolite, a number have been demonstrated to play a substantial role in cancer prevention,[1] immunomodulation,[2] plant tissue induction,[3] phytotoxicity,[4] fungus suppression,[5] malaria management,[6] biocontrol agent,[7] and mammalian intoxications.[8] Renewed understanding of the relevant molecular mechanisms of action of these compounds highlighted that the biochemical processes, in most cases, were fascinatingly unique.[9] Hence, trichothecenes have become a common research topic in the fields of medicine, agriculture, animal breeding, food safety, toxicology, and even biochemical antiterrorism, a field which is currently attracting much more public attention.

In our continuous characterization of chemically novel and/or biologically potent metabolites produced by fungi harboring in healthy plant tissues[10] or normal animal organs,[11] the presence of trichothecene metabolites was ascertained, prior to the detailed fractionation procedure, by ^{1}H NMR spectral analysis of extracts derived from a solid-substrate culture of *Myrothecium roridum* IFB-E009 and a liquid culture of *Myrothecium roridum* IFB-E012, which are endophytic fungi residing in two traditional Chinese medicinal plants, *Trachelospermum jasminoides* (Apocynaceae) and *Artemisia annua* (Asteraceae), respectively. Subsequent ^{1}H NMR monitored fractionation of the extracts led to the isolation of three new 10,13-cyclotrichothecane-based macrolides **1**–**3** in coexistence with the known analogues roridin E (**4**) and mytoxin B (**5**). The follow-up cytotoxicity assessment disclosed that the macrolides **1**–**5** were highly active against the human tumor cell line, nasopharyngeal epidermoid KB.

The stereospecificity is ubiquitous in biochemical processes, and some biological functions mainly result from chirality-dependent interactions between biomacromolecular targets and small-molecule substrates.[12] As for the trichothecenes with a diversity of biological functions, advanced knowledge about their absolute configuration could be a must for a better understanding and/or quantitative evalua-

[a] L. Shen, R. H. Jiao, Y. H. Ye, X. T. Wang, Dr. C. Xu, Dr. Y. C. Song, Prof. H. L. Zhu, Prof. R. X. Tan
Institute of Functional Biomolecules
State Key Laboratory of Pharmaceutical Biotechnology
Nanjing University, Nanjing 210093 (P. R. China)
Fax: (+86) 25-8330-2728
E-mail: zhuhl@nju.edu.cn
rxtan@nju.edu.cn

[†] Equally contributed to the work.

Supporting information for this article (Figures S1–S12 and Table S1) is available on the WWW under http://www.chemeurj.org/ or from the author.

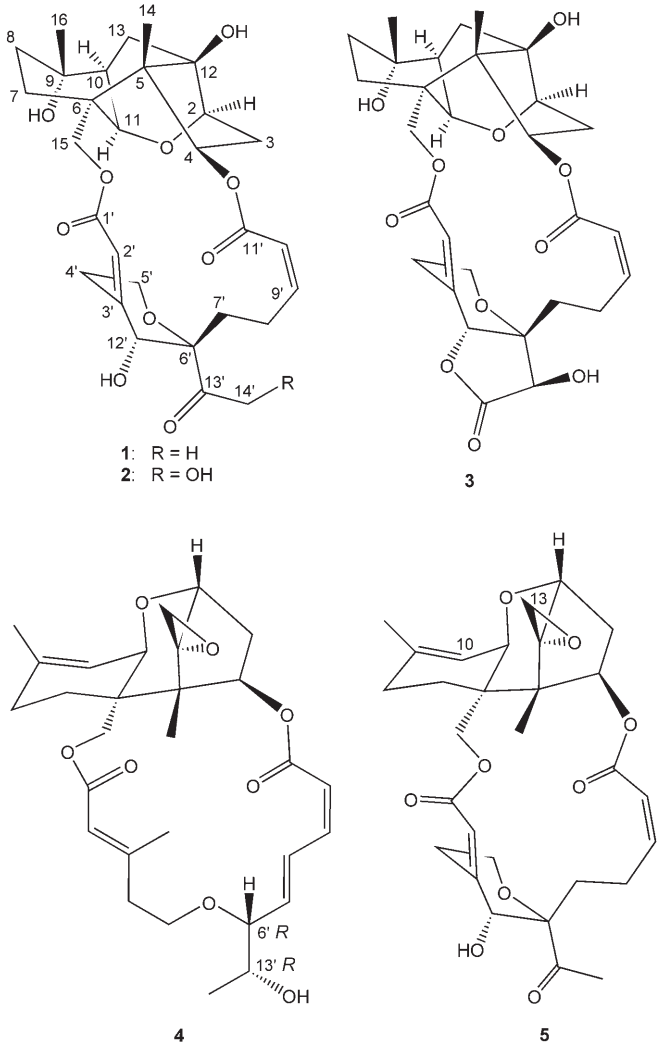

tions of the chiral specificity in functioning processes at the cellular and molecular level. This observation provided us with a strong impetus to assign the absolute configuration of new cytotoxic macrolides **1–3** and other structurally-related analogues by a combination of their CD data, Mosher's ester, and single-crystal X-ray diffraction analyses.

Results and Discussion

Myrothecine A (**1**) was isolated as colorless crystals. Its specific rotation was near to zero despite the multiple chiral centers present in its finally refined structure. The HRESI mass spectrum of **1** indicated that its molecular formula was $C_{29}H_{38}O_{10}$, necessitating a total of 11 degrees of unsaturation. The ^{1}H and ^{13}C NMR spectra of **1** displayed the coexistence of three methyls, nine methylenes, eight methines, six quaternary carbons, two double bonds, one ketone, and two ester carbonyls. This observation suggested that it was most likely a trichothecene compound belonging to the macrocyclic 10,13-cyclotrichothecane group.[1,13] This assumption was subsequently confirmed by a set of 2D NMR spectroscopic experiments (^{1}H–^{1}H COSY, NOESY, HMQC, and HMBC spectra) that provided data for the unequivocal assignment of all ^{1}H and ^{13}C NMR spectral data (Tables 1 and 2). In the ^{1}H–^{1}H COSY spectrum of **1**, the coupling sequences from H-2 through H-4, between H-7 and H-8, and of H-10 with H-11 and H-13 were readily recognized and connected to the sesquiterpenol moiety according to the HMBC correlations of (1) H-2 with C-4, C-5, and C-11, (2) H-3α with C-5 and C-12, (3) H-4 with C-5, C-6, and C-12, (4) H-11 with C-9 and C-15, and (5) H-15 with C-1′, C-7, and C-11. Furthermore, the chemical shifts from C/H-1′ through C/H-14′ were very close to those of mytoxin B,[14] indicating that they shared the same diacyl residue, situated at 4,15-oxygen atoms as demonstrated by the HMBC correlations of H-4 with C-11′ and H-15 with C-1′. Moreover, the formulated relative configuration of **1** was given by its NOESY spectrum which displayed the cross-peaks of (1) H-4 with H-3α, H-14, and H-15a, (2) H-11 with H-7α, H-10, and H-15a, (3) H-14 with H-7β, H-8β, and H-13β, (4) H-15a/b with H-4/H-7α, (5) H-16 with H-8β, H-10, and H-13β, and (6) H-2′ with H-7′a and H-12′. In addition, the assigned relative configuration of **1** was confirmed by single-crystal X-ray diffraction analysis (Figure 1).

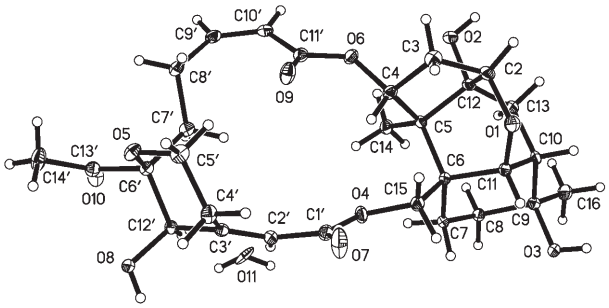

Figure 1. X-ray molecular structure of **1**.

The absolute configuration of **1** was determined by utilizing the NMR-tube Mosher's reactions,[15] taking advantage of the fact that the 12′-OH group could be acylated with the Mosher's reagent. The C-12′ atom was determined to have an *R* configuration (Figure 2) and the other chiral centers of **1** were, relative to the chirality of C-12′, assigned by single-crystal X-ray diffraction. The absolute configuration of **1** was established as 2*R*, 4*R*, 5*S*, 6*R*, 9*S*, 10*S*, 11*R*, 12*R*, 6′*S*, and 12′*R*.

Abstract in Chinese:

从两株内生真菌 *Myrothecium roridum* IFB-E009 和 IFB-E012（分别从络石 *Trachelospermum jasminoides*和黄花蒿*Artemisia annua*分到)的发酵产物中得到三个新的具细胞毒活性的10,13-环单端孢霉烷型大环内酯myrothecines A-C (**1-3**)。采用将二维NMR、CD等多种光谱技术兼与核磁管内的Mosher反应和单晶衍射分析相关联的方法测定了新化合物**1-3**和已知类似物mytoxin B (**5**)的绝对构型。此外，本文还简要讨论了这些新大环内酯成分的发现在内共生和生物催化方面的潜在意义。

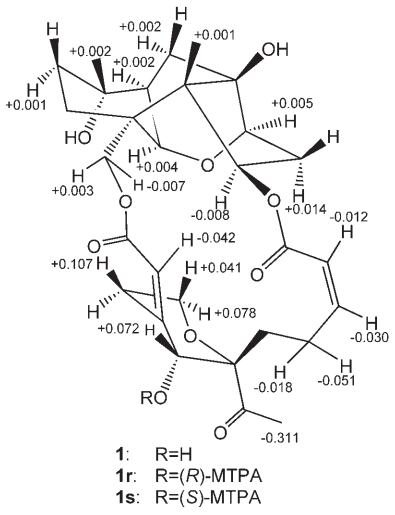

Figure 2. $\Delta\delta$ ($=\delta_S-\delta_R$, expressed in ppm) values obtained for the MTPA esters of **1**. MTPA = Methoxy(trifluoromethyl)phenylacetic acid.

The crystal structure of **1** (Figure 1) is orthorhombic with the space group $P2_12_12$. The 16-membered ring in each molecule consists of two α,β-unsaturated esters with the two carbonyls on the same side of the macrocycle. A tetrahydropyran ring in a chair conformation consisting of C3′, C4′, C5′, O5, C6′, and C12′ is enwrapped inside the macrocycle. The acetyl and hydroxyl groups on the ring are positioned on the side of the "chair" that is oriented towards the outside of the 16-membered cycle, creating a space insufficient to accommodate small-molecule solvents, such as methanol. The length of each molecule of **1** is about 15.4 Å, indicating that **1** is a nano-sized molecule, which is combined via intermolecular hydrogen bonding to form 2D-layers along the *ab* plane (Figure S11).

The molecular formula of myrothecine B (**2**) was determined as $C_{29}H_{38}O_{11}$, with one extra oxygen atom than that of **1**, from its HRESI mass spectrum. Furthermore, the ^{1}H and ^{13}C NMR spectra of **2** were comparable to those of **1** with most of the data being nearly identical in both sets (Tables 1 and 2). However, clear NMR spectral differences could be readily recognized as the following: the 14′-methyl singlet ($\delta_H = 2.30$ ppm) in the ^{1}H NMR spectrum of **1** was replaced by a pair of mutually coupled doublets ($J = 20.2$ Hz) at $\delta_H = 4.58$ and 4.39 ppm. This observation, particularly the big geminal coupling constant of the 14′-methylene protons, required the presence of a hydroxyacetyl group.[1,16] This could be rationalized by assuming that **2** was a 14′-hydroxylated derivative of **1**, which was confirmed by the ^{13}C NMR spectrum of **2** in which an oxygenated methylene carbon signal at $\delta_C = 69.2$ ppm substituted for the 14′-methyl resonance at $\delta_C = 28.7$ ppm in that of **1**. Moreover, the structure proposed for **2** was reinforced by its ^{1}H–^{1}H COSY, NOESY, HMQC, and HMBC spectra resulting in the unequivocal assignment of its ^{1}H and ^{13}C NMR spectral data (Tables 1 and 2) and the relative configuration of **2**. Finally, myrothecine B (**2**) was shown to share the same absolute configuration (2*R*, 4*R*, 5*S*, 6*R*, 9*S*, 10*S*, 11*R*, 12*R*, 6′*S*, and 12′*R*) with myrothecine A (**1**) by the close resemblance in their ^{13}C NMR spectral data (except for C-14′, Table 2). This allocation was reinforced by its CD spectrum, which exhibited the negative and positive Cotton effects at $\lambda_{max} = 232$ and 247 nm (nearly identical to those of **1**, Figure S1a and b) arising from $\pi\rightarrow\pi^*$ and $n\rightarrow\pi^*$ transitions of the γ-chiral α,β-unsaturated ester chromophore, respectively.

The molecular formula of myrothecine C (**3**) was determined as $C_{29}H_{36}O_{11}$, two hydrogens less than that of myrothecine B (**2**), from its HRESI mass spectrum. This observa-

Table 1. ^{1}H NMR spectroscopic data for compounds **1**, **2**, and **3** δ/ppm (multiplicity, *J*/Hz).

Proton	**1**[a]	**2**[b]	**3**[c]
2	3.99 (d, 4.1)	3.88 (d, 3.9)	3.80 (d, 3.7)
3α	2.39 (br dd, 15.6, 8.0)	2.1 (m)	2.13 (dd, 15.2,8.0)
3β	1.84 (ddd, 15.6, 3.8, 2.9)	1.85 (m)	1.70 (m)
4	5.16 (dd, 7.9, 2.4)	5.15 (dd, 8.0, 3.0)	5.06 (d, 6)
7α	1.55 (ddd, 14.5, 14.0, 5.4)	1.55 (m)	1.40 (td, 14.3, 5.0)
7β	2.15 (m)	2.15 (m)	1.97 (d, 12.6)
8α	1.39 (br dd, 14.5, 4.9)	1.35 (br dd, 14.3, 5.2)	1.23 (br d, 14.3)
8β	1.77 (ddd, 14.5, 14.0, 4.9)	1.80 (m)	1.58 (td, 14.0,4.3)
10	2.18 (m)	2.10 (m)	2.00 (br d, 11.3)
11	3.61 (d, 3.6)	3.57 (d, 4.0)	3.46 (d, 3.3)
13α	1.93 (dd, 13.9, 12.0)	1.85 (m)	1.72 (m)
13β	1.46 (dd, 13.9, 5.4)	1.55 (m)	1.32 (dd, 13.8, 5.3)
14	1.10 (s)	1.14 (s)	0.94 (s)
15a	4.54 (d, 11.7)	4.51 (d, 11.6)	4.36 (br d, 11.6)
15b	3.65 (d, 11.7)	3.56 (d, 11.6)	3.54 (br d, 11.6)
16	1.24 (s)	1.18 (s)	1.05 (s)
2′	5.78 (br s)	5.94 (br s)	5.79 (s)
4′α	2.75 (dddd, 13.3,12.5,6.6, 1.5)	2.79 (m)	2.39 (dd, 12.6, 5.7)
4′β	3.53 (br d, 13.3)	3.47 (br d, 13.0)	3.37 (br d, 12.9)
5′α	4.05 (br dd, 11.5, 6.2)	3.96 (m)	3.73 (dd, 10.8, 5.5)
5′β	4.19 (td, 11.5, 2.7)	4.18 (td, 11.2, 2.7)	4.07 (t, 11.0)
7′a	1.96 (m)	2.05 (m)	1.71 (m)
7′b	1.65 (m)	1.70 (m)	1.53 (ddd, 14, 8.9, 4.2)
8′a	2.82 (m)	2.79 (m)	2.72 (m)
8′b	1.69 (ddd, 12.9, 9.2, 3.6)	1.65 (m)	1.79 (m)
9′	6.42 (ddd, 11.6, 9.2, 6.3)	6.46 (m)	6.35 (m)
10′	5.76 (dd, 11.6, 2.0)	5.81 (dd, 11.6, 2.4)	5.67 (d, 11.3)
12′	3.97 (br s)	3.96 (br s)	4.31 (s)
13′			3.62 (s)
14′a	2.30 (s)	4.58 (d, 20.2)	
14′b		4.39 (d, 20.2)	

[a] Spectra recorded at 500 MHz in $CDCl_3$. [b] Spectra recorded at 300 MHz in [D_6]acetone. [c] Spectra recorded at 500 MHz in $CDCl_3$/[D_6]DMSO 6:1.

Table 2. ^{13}C NMR spectroscopic data for compounds **1**, **2**, and **3** δ/ppm.

Carbon	**1**[a]	**2**[b]	**3**[c]
2	80.8	81.7	80.4
3	40.4	41.3	39.9
4	79.3	79.4	78.4
5	51.2	52.0	50.8
6	44.0	44.5	43.5
7	28.3	29.0	27.8
8	31.3	31.9	30.7
9	73.6	74.1	72.3
10	44.2	45.1	43.7
11	69.0	70.0	68.9
12	78.1	77.3	76.5
13	28.1	29.3	28.2
14	10.4	10.9	10.1
15	73.0	73.0	73.0
16	28.1	27.9	27.3
1′	165.5	166.6	164.8
2′	117.3	117.4	118.9
3′	154.1	156.1	148.5
4′	25.5	26.3	25.0
5′	63.0	63.7	64.4
6′	87.3	88.5	83.0
7′	29.5	30.7	23.5
8′	21.3	21.7	20.8
9′	148.0	147.6	147.8
10′	120.8	122.4	120.7
11′	165.8	167.2	165.7
12′	77.3	77.7	84.0
13′	213.0	213.4	72.2
14′	28.7	69.2	175.9

[a] Spectra recorded at 125 MHz in $CDCl_3$. [b] Spectra recorded at 75 MHz in [D_6]acetone. [c] Spectra recorded at 125 MHz in $CDCl_3$/[D_6]DMSO 6:1.

tion, along with the ^{1}H and ^{13}C NMR spectra of **3**, suggested that it was a congener of metabolites **1** and **2**. Furthermore, the ^{1}H and ^{13}C NMR signals of **3**, except for those from H/C-12′ through H/C-14′ were comparable to those of **1** and **2**, highlighting that it was only different from the two metabolites in the functionality of positions 12′–14′. This assumption was confirmed by its ^{1}H–^{1}H COSY, NOESY, HMQC, and HMBC spectra permitting the exact assignment of all ^{1}H and ^{13}C NMR spectral data (Tables 1 and 2). In particular, the H-12′ singlet of **3** at $\delta_H = 4.31$ ppm was observed to be substantially downfield relative to those (around $\delta_H =$ 3.96 ppm) of **1** and **2**, and the H-14′ signals discerned with **1** and **2** were replaced by a one-proton singlet of **3** at $\delta_H =$ 3.62 ppm. In the ^{13}C NMR spectrum of **3**, the resonance lines due to C-3′, 6′, 7′, 12′, 13′, and 14′ were remarkably deviated from those of **1** and **2**. These spectral features, along with the unsaturation index of **3**, demonstrated the presence of an α-hydroxy γ-lactone. The formulated relative configuration of **3** was established by its NOESY spectrum and single-crystal X-ray diffraction analysis. The absolute configuration of **3** was determined to be 2*R*, 4*R*, 5*S*, 6*R*, 9*S*, 10*S*, 11*R*, 12*R*, 6′*S*, 12′*R*, and 13′*R* (Figure 3) by the close resemblance of its ^{1}H and ^{13}C NMR spectral data, due to the seaquiterpenol moiety of **3**, to those of metabolites **1** and **2**. The CD spectrum of **3** was also comparable to that of **1** and **2**, although the intensity of its positive Cotton effect at

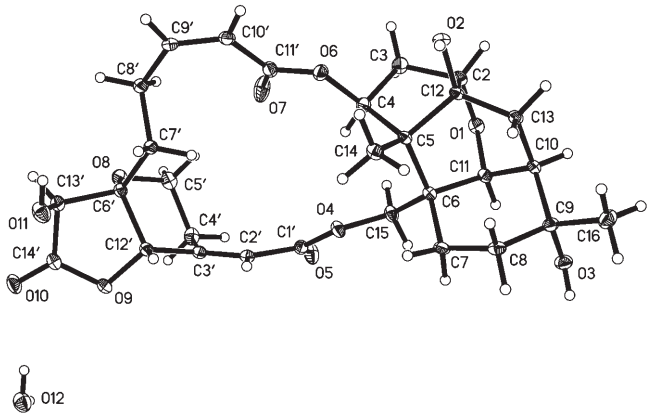

Figure 3. X-ray molecular structure of **3**.

251 nm ascribable to the $n \rightarrow \pi^*$ transition of the γ-chiral α,β-unsaturated ester chromophore was deceased substantially as a result of the electron-withdrawing effect of the γ-lactone carbonyl on the 12′-oxygen atom (Figure S1c).

It was noteworthy that myrothecine C (**3**) also possesses a 16-membered macrocycle, the size of which is about 5 × 7 Å^2. The two ester carbonyls are located at the same side of the macrocycle. No H_2O or other small solvent molecules were embedded in the macrocycle, although the cycle did create a space big enough to host such molecules. If correlated with the macrocyle size of **1** (see above), it could be hypothesized that the rigidity of the lactone ring could influence the conformation of the macrocyle. Furthermore, all the hydroxyls, carboxyl oxygens (except O-7), and H_2O molecules contributed to intermolecular hydrogen bonding (O-12–H···O-5, $a = 2.988(3)$ Å; O-12–H···O-3, $b = 2.912(2)$ Å; O-11–H···O-5, $c = 2.912(2)$ Å; O-3–H···O-2, $d = 2.884(2)$ Å; and O-2–H···O-12, $e = 2.835(2)$ Å). Most of the angles were larger than 160°, indicating a strong hydrogen bond. Through multiple hydrogen bonds, the molecules of **3** and water joined to form the observed three-dimensional structure (Figure S12).

The MS and ^{1}H/^{13}C NMR spectra of metabolite **4** established its identity as roridin E, with its absolute configuration unambiguously assigned elsewhere.[8] The metabolite **5**, the most cytotoxic to the KB cell line, was ascertained to be mytoxin B by comparing its MS and ^{1}H/^{13}C NMR spectral data with those in the literature.[14] However, no report dealing with the assignment of its absolute configuration could be found. As a matter of fact, the close resemblance of its ^{1}H and ^{13}C NMR spectral data ($\Delta\delta_H = < 0.2$ ppm, $\Delta\delta_C = < 1.0$ ppm, except for the shift deviation created by the difference in the acyl moieties) with those of roridin E (**4**) and verrucarin A indicated that metabolite **5** shared with **4** and verrucarin A the same sesquiterpenol residue with its absolute configuration assigned as 2*R*, 4*R*, 5*S*, 6*R*, 11*R*, and 12*R*.[8,17] A close comparison of the ^{13}C NMR spectra of **5** and **1** demonstrated that the resonance lines from C-1′–C-14′ were identical in both sets. This observation substantiated that the absolute configuration of the diacyl moiety was

6′*S* and 12′*R*. This assumption was reinforced by the CD spectrum of **5**, which gave negative and positive Cotton effects at $\lambda_{max}=233$ and 248 nm, respectively, nearly identical to those of **1** and **2** (Figures S1a, b, and d). In conclusion, the absolute configuration of mytoxin B was elucidated as 2*R*, 4*R*, 5*S*, 6*R*, 11*R*, 12*R*, 6′*S*, and 12′*R*.

The in vitro cytotoxicity of the macrolides **1**–**5** was evaluated against the human tumor cell line nasopharyngeal epidermoid KB. All the macrolides showed significant cytotoxicity with the corresponding IC_{50} (the inhibition concentration at which 50% survival of cells was allowed) values of 8.5 (15.6), 0.76 (1.4), 32.21 (57.5), 0.034 (0.066), and 0.0022 $\mu g\,mL^{-1}$ (0.0042 μM), respectively. The IC_{50} value of 5-fluorouracil (a clinically prescribed antitumor drug coassayed as a positive control) against the three tumor cell lines was 1.82 $\mu g\,mL^{-1}$ (14 μM).

Conclusion

The present work characterized three new 10,13-cyclotrichothecane-derived macrolides **1**–**3** from cultures of two endophytic *Myrothecium roridum* strains, IFB-E009 and IFB-E012. Previously, macrocyclic analogues of this skeleton with different acylation patterns were isolated from cultures of *Calcarisporium arbuscula* (harboring in the fruiting body of the mushroom *Ganoderma lucidum* collected in the Sichuan Province of China)[13] and *Myrothecium verrucaria* associated with the sponge *Spongia* sp. (collected off the coast of Maui, Hawaii).[1] Even earlier, 10,13-cyclotrichothecane-derived macrolides were found as secondary metabolites of *M. verrucaria* obtained from the roots of *Baccharis coridifolia*.[18] Chemically, 12,13-epoxytrichothec-9-enes could be rearranged into 10,13-cyclotrichothecane derivatives upon boiling in the presence of a weak acid.[19] However, few reports were available describing the direct characterization of 10,13-cyclotrichothecane-based metabolites from any culture of environmental microbes. Moreover, the 12,13-epoxytrichothec-9-ene metabolites seemed to be more active than the corresponding rearranged products with a 10,13-cyclotrichothecane skeleton.[1,19] This observation suggested 10,13-cyclotrichothecane-derived macrolides could be related to the endophytism and/or symbiosis in which a detoxication process could result from the host-microbe interadaptation initiated through several mechanisms, such as expoxide hydrolase, which was reported to be involved in plant-fungus interactions.[20] In correlation to this fact, the detection of the 10,13-cyclotrichothecane macrolides from the endophyte cultures highlights the possibility that *Myrothecium roridum* strains IFB-E009 and IFB-E012 could be a new source of fungal epoxide hydrolase(s), which are of high value for microbiological transformations.[21]

Experimental Section

General: Melting points were measured on an XT-4 apparatus and are uncorrected. Optical rotation was determined in MeOH on a WXG-4 disc polarimeter, and IR spectra by using KBr disks on a Nexus 870 FTIR spectrometer. UV spectra were recorded on a Hitachi U-3000 spectrophotometer. NMR spectra were acquired on Bruker DRX-500 and DPX-300 NMR spectrometers by using TMS and solvent signals as internal standards. ESIMS and HRESIMS were taken on a Mariner Mass 5304 instrument. CD spectra were recorded on a Jasco J-810 circular dichroism spectrometer. Silica gel (200–300 mesh) for column chromatography and silica GF_{254} for TLC were produced by Qingdao Marine Chemical Company (China). Sephadex LH-20 was purchased from Pharmacia Biotech (Sweden). ODS silica gel was obtained from Nacalai Tesque, Kyoto (Japan). The ELISA plate reader was obtained from Sunrise (USA). Mosher's acid chloride was purchased from Aldrich. HPLC analyses were performed by using a column of Allsphere ODS-2.5 μm (250×4.6 mm), Hitachi pump L-7100, and a UV detector L-7400. All chemicals used in the study were of analytical grade.

Microorganisms: Following the procedure previously detailed,[22] the strains IFB-E009 and IFB-E012 were isolatedfrom surface-sterilized stems of apparently healthy *T. jasminoides* and *A. annua*, respectively, the former of which was collected in March 2002 from the Zijin Mountain in the suburb of Nanjing (China) and the latter collected in May 2003 from the coast of the Yangtze River in the same city. Both strains were identified by comparing the morphological character and 18S rDNA sequence with those of standard records. Specifically, the morphological examination was performed by scrutinizing the fungal culture, the mechanism of spore production, and the characteristics of the spores. For inducing sporulation, each of the isolated fungal strains was separately inoculated on PDA, CMA, CA, WSA, and PCA in Petri dishes. All experiments and observations were repeated at least twice leading to the coidentification of the two strains as *Myrothecium roridum*,[23] which were kept at the Institute of Functional Biomolecules, Nanjing 210093 (China).

Fermentation: *M. roridum* IFB-E009 was cultured by a solid-matrix steady protocol, which we have previously described.[24] Briefly, the fresh mycelium grown on potato-detrose agar (PDA) medium at 28°C for 5 days was inoculated into Erlenmeyer flasks (1000 mL) containing PD medium (400 mL). After 6 days of incubation at 28°C on a rotary shaker at 150 rpm, the liquid culture (20 mL) was transferred as the seed into 500 bottles preloaded with a given amount of grain medium composed of grain (7.5 g), bran (7.5 g), yeast (0.5 g), sodium tartrate (0.1 g), $FeSO_4{\cdot}7H_2O$ (0.01 g), sodium glutamate (0.1 g), pure corn oil (0.1 mL), and water (30 mL). Cultivation was kept for 45 days at 28°C.

M. roridum IFB-E012 was cultured in liquid medium. The fresh mycelium grown on PDA medium at 28°C for 5 days was inoculated into flasks (1000 mL) containingCzapek's medium (500 mL from a mixture of sucrose (30 g), $NaNO_3$ (3 g), K_2HPO_4 (1 g), yeast extract (1 g), KCl (0.5 g), $MgSO_4{\cdot}7H_2O$ (0.5 g), $FeSO_4$ (0.01 g), and H_2O (1000 mL)). After 5 days of the incubation at 28°C on a rotary shaker at 150 rpm, a portion of the liquid culture (50 mL) was transferred as the seed into each of a total of 300 flasks (1000 mL) containing Czapek's medium (500 mL). The liquid cultivation that followed was kept for 10 days at 28°C and 150 rpm on a rotary shaker.

Extraction and isolation: The culture filtrates of *M. roridum* IFB-E012 (total volume 165 L) was extracted exhaustively with EtOAc. Evaporation of the solvent from the extract in vacuo yielded a black residue (35 g). After eliminating waxy substances, a residue (27 g) was obtained, which was then chromatographed over silica gel (160 g) eluting successively with $CHCl_3$/MeOH 100:0→0:100. Based on the TLC monitoring, the collected fractions (500 mL each) were combined into six parts. Fraction-2 was purified by column chromatography fractionation over silica gel with $CHCl_3$/MeOH 100:0→100:16. Gel filtration of Fraction-2–2 over Sephadex LH-20 with $CHCl_3$/MeOH 1:1 followed by ODS silica gel column chromatography eluting with H_2O/MeOH 100:0→60:40 produced compound **1** (65 mg). Fraction-2–3 was purified by using Sephadex LH-20 with $CHCl_3$/MeOH 1:1 and then further purified by HPLC with

MeOH/H_2O 65:35 (0.7 mL min^{-1}) to yield roridin E (**4**) (3 mg, t_R = 25 min) and mytoxin B (**5**, 12 mg, t_R = 15 min). Fraction-4 was also purified by column chromatography fractionation over silica gel with $CHCl_3$/MeOH 100:1→100:16 and the obtained fractions 4–3 were purified by HPLC with MeOH/H_2O 35:65 (0.6 mL min^{-1}) to provide **2** (4 mg, t_R = 19.2 min).

Crude MeOH extract (327 g) of a solid culture of *M. roridum* IFB-E009 was fractionated after preliminary treatment as described above. The obtained fraction-4 was purified by silica gel column chromatography eluting with $CHCl_3$/MeOH 100:1→100:8, and then fraction-4–6 was further purified by using Sephadex LH-20 repeatedly with $CHCl_3$/MeOH 1:1 as the eluent. Finally, repetitive recrystallization by using $CHCl_3$/MeOH 1:1 at room temperature provided myrothecine **3** as colorless crystals (15.5 mg). ^{1}H and ^{13}C NMR spectroscopic data for myrothecines A–C are listed in Tables 1 and 2

Myrothecine A (1): Colorless crystals; m.p. 252–254 °C; $[\alpha]_D^{25}$ = 0.0 (c = 0.00436 in MeOH); UV (MeOH): λ_{max} (ε) = 214 nm (19400 mol^{-1} dm^3 cm^{-1}); CD (CH_3OH): λ_{max} ($\Delta\varepsilon$) = 232 (−0.47), 246 nm (0.42 mol^{-1} dm^3 cm^{-1}); IR (KBr): $\tilde{\nu}$ = 3444, 3303, 2930, 1714, 1663, 1635, 1413, 1400, 1254, 1235, 1203, 1174, 1159, 1051, 1031, 929, 817, 776 cm^{-1}; HRESIMS: m/z: calcd for $C_{29}H_{38}O_{10}Na$: 569.2357; found: 569.2356 $[M+Na]^+$.

Myrothecine B (2): Colorless crystals; m.p. 213–216 °C; $[\alpha]_D^{25}$ = +0.6 (c = 0.00053 in MeOH); UV (MeOH): λ_{max} (ε) = 219 nm (9900 mol^{-1} dm^3 cm^{-1}); CD (CH_3OH): λ_{max} ($\Delta\varepsilon$) = 232 (−0.61), 247 nm (0.42 mol^{-1} dm^3 cm^{-1}); IR (KBr): $\tilde{\nu}$ = 3403, 2959, 1716, 1661, 1639, 1412, 1396, 1251, 1222, 1191, 1156, 1057, 1024, 764 cm^{-1}; HRESIMS: m/z: calcd for $C_{29}H_{38}O_{11}Na$: 585.2306; found: 585.2296 $[M+Na]^+$.

Myrothecine C (3): Colorless crystals; m.p. 220–223 °C; $[\alpha]_D^{25}$ = +7.3 (c = 0.001 in MeOH); UV (MeOH): λ_{max} (ε) = 223 nm (12300 mol^{-1} dm^3 cm^{-1}); CD (CH_3OH): λ_{max} ($\Delta\varepsilon$) = 232 (−2.96), 251 nm (0.46 mol^{-1} dm^3 cm^{-1}); IR (KBr): $\tilde{\nu}$ = 3338, 2901, 1642, 1428, 1369, 1335, 1316, 1281, 1203, 1156, 1103, 1048, 998, 898, 701, 664, 608, 518, 457, 436 cm^{-1}; HRESIMS: m/z: calcd for $C_{29}H_{36}O_{11}Na$583.2150; found: 583.2143 $[M+Na]^+$.

Single-crystal X-ray diffractions: Determination of the crystal structures of myrothecines A (**1**) and C (**3**) was carried out on a Nonius CAD4 diffractometer equipped with graphite-monochromated $Mo_{K\alpha}$ radiation (λ = 0.71073), and with Lorentz polarization and absorption corrections for a crystal of the title compounds (0.25×0.25×0.18 mm for **1** and 0.27×0.20×0.18 mm for **3**). The intensities were collected at 293 K by using a ω-scan mode with variable scan speed. A total of 17638 reflections for **1** (and 12343 reflections for **3**) were collected in the range of θ = 1.53–28.36° for **1** (θ = 2.67–28.32° for **3**) of which 6594 for **1** (6418 for **3**) were independent. For **1**, 4855 (5722 for **3**) observable reflections with $I \geq 2\sigma(I)$ were used in the structure solution and refinements. The structure was solved by direct methods and refined on F^2 by full-matrix least-squares methods by using SHELX-97.[25] All the non-hydrogen atoms were refined anisotropically. All the hydrogen atoms were placed in calculated positions and were assigned fixed isotropic thermal parameters at 1.2 times the equivalent isotropic U of the atoms to which they are attached and allowed to ride on their respective parent atoms. The contributions of these hydrogen atoms were included in the structure-factors calculations. The refinement gave the final R_1 = 0.074 for **1** (R_1 = 0.042 for **3**) with $w = [\sigma^2(F_o)^2 + (0.1(\max(0,F_o^2) + 2F_c^2)/3)^2]^{-1}$. Some crystallographic and experimental data for the two compounds are listed in Table S1.[26]

Preparation of (*R*)- and (*S*)-MTPA Esters (1r and 1s): Myrothecine A (**1**) was dissolved in [D_5]pyridine in an NMR tube, and then dried under a nitrogen stream. A baseline ^{1}H NMR spectrum was then recorded as a reference, followed by the addition of a calculated amount of (*R*)-MTPA chloride into the NMR tube. This tube was rigorously shaken to afford even mixing. The NMR tube was maintained at room temperature for 12 h until the acylation reaction had gone to completion. The ^{1}H NMR spectrum was recorded every 4 h and a ^{1}H–^{1}H COSY spectrum of the resulting (*S*)-MTPA ester (**1s**) was recorded. Similarly, **1** was acylated with (*S*)-MTPA chloride to generate the (*R*)-MTPA ester (**1r**), and the ^{1}H–^{1}H COSY spectrum of the obtained (*R*)-MTPA ester (**1r**) was also recorded.[15,27]

Cytotoxicity assay: The in vitro cytotoxicity was evaluated as described in our previous paper.[10]

Acknowledgements

The work was cofinanced by grants for R.X.T. (Projects 20432030 & 30570010) from National Natural Science Foundation of China.

[1] T. Amagata, C. Rath, J. F. Rigot, N. Tarlov, K. Tenney, F. A. Valeriote, P. Crews, *J. Med. Chem.* **2003**, *46*, 4342–4350.
[2] G. S. Bondy, J. J. Pestka, *J. Toxicol. Environ. Health B Crit. Rev.* **2000**, *3*, 109–143.
[3] A. Kobayashi, Y. Nakae, T. Kawasaki, K. Kawazu, *Agric. Biol. Chem.* **1989**, *53*, 585–590.
[4] a) H. K. Abbas, B. B. Johnson, W. T. Shier, H. Tak, B. B. Jarvis, C. D. Boyette, *Phytochemistry* **2002**, *59*, 309–313; b) A. Shimada, S. Takeuchi, M. Kusano, S. Fujioka, Y. Kimura, *Plant Sci.* **2004**, *166*, 1307–1312; c) A. Andolfi, A. Boari, A. Evidente, M. Vurro, *J. Agric. Food Chem.* **2005**, *53*, 1598–1603.
[5] T. Sugawara, A. Tanaka, K. Nagai, K. Suzuki, G. Okada, *J. Antibiot.* **1997**, *50*, 778–780.
[6] M. Isaka, J. Punya, Y. Lertwerawat, M. Tanticharoen, Y. Thebtaranonth, *J. Nat. Prod.* **1999**, *62*, 329–331.
[7] K. F. Nielsen, T. Gräfenhan, D. Zafarri, U. Thrane, *J. Agric. Food Chem.* **2005**, *53*, 8190–8196.
[8] B. B. Jarvis, S. J. Wang, *J. Nat. Prod.* **1999**, *62*, 1284–1289.
[9] a) S. Kinser, M. Li, Q. S. Jia, J. J. Pestka, *J. Nutr. Biochem.* **2005**, *16*, 88–95; b) S. P. McCormick, L. J. Harris, N. J. Alexander, T. Ouellet, A. Saparno, S. Allard, A. E. Desjardins, *Appl. Environ. Microbiol.* **2004**, *70*, 2044–2051; c) J. J. Pestka, H. -R. Zhou, Y. Moon, Y. J. Chung, *Toxicol. Lett.* **2004**, *153*, 61–73; d) E. J. Chung, K. Choi, H. W. Kim, D. H. Lee, *Biol. Pharm. Bull.* **2003**, *26*, 32–36.
[10] L. Shen, Y. H. Ye, X. T. Wang, H. L. Zhu, C. Xu, Y. C. Song, H. Li, R. X. Tan, *Chem. Eur. J.* **2006**, in press.
[11] J. Y. Liu, L. L. Huang, Y. H. Ye, W. X. Zou, Z. J. Guo, R. X. Tan, *J. Appl. Microbiol.* **2006**, *100*, 195–202.
[12] a) J. Grimsby, R. Sarabu, W. L. Corbett, N. E. Haynes, F. T. Bizzarro, J. W. Coffey, K. R. Guertin, D. W. Hilliard, R. F. Kester, P. E. Mahaney, L. Marcus, L. D. Qi, C. L. Spence, J. Tengi, M. A. Magnuson, C. A. Chu, M. T. Dvorozniak, F. M. Matschinsky, J. F. Grippo, *Science* **2003**, *301*, 370–373; b) M. Hamberg, *FEBS J.* **2005**, *272*, 736–743; c) G. Pinna, E. Costa, A. Guidotti, *Proc. Natl. Acad. Sci. USA* **2004**, *101*, 6222–6225.
[13] N. J. Yu, S. X. Guo, P. G. Xiao, *Acta Bot. Sin.* **2002**, *44*, 878–882.
[14] B. B. Jarvis, F. T. Çömezoğlu, Y. W Lee, J. L. Flippen-Anderson, R. D. Gilardi, C. F. Geoge, *Bull. Soc. Chim. Belg.* **1986**, *95*, 681–697.
[15] R. X. Tan, P. R. Jensen, P. G. Williams, W. Fenical, *J. Nat. Prod.* **2004**, *67*, 1374–1382.
[16] K. A. Alvi, J. Rabenstein, J. Woodard, D. D. Baker, J. D. Bergthold, J. Lynch, K. L. Lieu, I. A. Braude, *J. Nat. Prod.* **2002**, *65*, 742–744.
[17] M. Matsumoto, H. Minato, K. Tori, M. Ueyama, *Tetrahedron Lett.* **1977**, *18*, 4093–4096.
[18] G. Habermehl, *Pure Appl. Chem.* **1989**, *61*, 377–380.
[19] J. F. Grove, *J. Chem. Soc. Perkin Trans. 1* **1986**, 647–654.
[20] K. Gomi, H. Yamamato, K. Akimitsu, *Plant Mol. Biol.* **2003**, *53*, 189–199.
[21] P. Moussou, A. Archelas, R. Furstoss, *J. Mol. Catal. B: Enzym.* **1998**, *5*, 447–458.
[22] H. Lu, W. X. Zou, J. C. Meng, J. Hu, R. X. Tan, *Plant Sci.* **2000**, 151, 67–73.
[23] a) I. Larena, O. Salazar, V. Gonzalez, M. C. Julian, V. Rubio, *J. Biotechnol.* **1999**. *75*, 187–194; b) T. J. White, T. Bruns, S. Lee, J. Taylor, *Amplification and direct sequencing of fungal ribosomal RNA genes for phylogenetics. PCR Protocols: A Guide to Methods and Application*, Academic Press, San Diego, CA, **1990**, pp. 315–322.

[24] J. Y. Liu, Y. C. Song, Z. Zhang, L. Wang, Z. J. Guo, R. X. Tan, *J. Biotechnol.* **2004**, 114, 279–287.
[25] G. M. Sheldrick, SHELX-97, Program for X-ray Crystal Structure Solution and Refinement, Göttingen University, Germany, **1997**.
[26] CCDC-295224 (for myrothecine A, **1**) and -295223 (for myrothecine C, **3**) contain the supplementary crystallographic data for this paper. These data can be obtained free of charge from the Cambridge Crystallographic Data Centre via www.ccdc.cam.ac.uk/data_request/cif.
[27] I. Ohtani, T. Kusumi, Y. Kashman, H. Kakisawa, *J. Am. Chem. Soc.* **1991**, *113*, 4092–4096.

Received: January 19, 2006
Published online: May 4, 2006

